The Journal of Immunology

RESEARCH ARTICLE | MARCH 15 2004

Targeted Bioactivity of Membrane-Anchored TNF by an Antibody-Derived TNF Fusion Protein[1] FREE

Stefan Bauer; ... et. al

J Immunol (2004) 172 (6): 3930–3939.
https://doi.org/10.4049/jimmunol.172.6.3930

Targeted Bioactivity of Membrane-Anchored TNF by an Antibody-Derived TNF Fusion Protein[1]

Stefan Bauer,* Nicole Adrian,* Barbara Williamson,† Con Panousis,‡ Natalie Fadle,* Joanna Smerd,* Ilknur Fettah,* Andrew M. Scott,‡ Michael Pfreundschuh,* and Christoph Renner[2]*

We describe the generation and characterization of a fusion protein consisting of a humanized anti-fibroblast-activating protein (anti-FAP) Ab and human TNF replacing the IgG1 CH2/CH3 Fc domain. The construct was generated by recombinant DNA technology and preserved its IgG1-derived dimeric structure with the TNF molecule linked as a dimer. Expression in CHO cells was optimized in serum-free medium under GMP conditions to achieve production levels up to 15 mg/liter. Recognition of the FAP Ag by the construct was as good as that by the parental anti-FAP Ab. TNF signaling was induce able via both TNF receptor types. When acting in solution, the Ab-linked TNF dimer exhibited a 10- to 20-fold lower activity compared with recombinant trimeric TNF. However, after binding to FAP-expressing cells, immobilized anti-FAP-TNF dimer was equivalent to membrane-anchored TNF with regard to bioactivity. Amplification of TNF-related pathways by mimicking the membrane-integrated TNF signaling was detectable in various systems, such as apoptosis induction or tissue factor production. The difference in TNF receptor type 1 and 2 signaling by the anti-FAP-TNF construct correlated well with its Ag-bound or -soluble status. Translating the approach into a xenograft animal model (BALB/c *nu/nu* mice), we demonstrated low toxicity with measurable antitumor efficacy for the TNF fusion protein after i.v. application. Immunohistochemical analysis of tumor sections showed restricted TNF-mediated macrophage recruitment to the targeted tissue in a time- and dose-dependent manner. These data warrant transfer of the anti-FAP-TNF immunocytokine into clinical trials for the treatment of FAP-positive tumors. ***The Journal of Immunology*****, 2004, 172: 3930–3939.**

Tumor necrosis factor is expressed by numerous cell types as a 26-kDa, type II transmembrane TNF (memTNF)[3] and as a soluble 17-kDa form (sTNF), which results from proteolytic cleavage of memTNF (1, 2). TNF signals are transduced by two different plasma membrane receptors, TNFRSF1A (TNF receptor superfamily, member 1A; p60; TNF-R1) and TNFRSF1B (TNF receptor superfamily, member 1B; p80; TNF-R2) (3). Although most cell lines and primary tissues coexpress both receptor types, cellular responses to the soluble 17-kDa component are mediated by the interaction with TNF-R1 (4). In addition to its role as a major mediator of inflammatory responses and immune cell proliferation, sTNF is also involved in the lysis of infected or transformed cells (5). In contrast to the systemic activity of sTNF, memTNF exerts its cytotoxic effects in a locally restricted manner, because it depends on direct cell-to-cell contact (6). After appropriate stimulation, human monocytes, macrophages, and $CD8^+$ T cells present membrane-anchored TNF as a key component in their cytolytic pathways (7, 8). Although memTNF acts predominantly via TNF-R2, it can potently trigger both receptor types (9), leading to a positive cooperative receptor cross-talk (10). This agonistic triggering of TNF-R2 is not only a simple additive effect to TNF-R1 signaling, but can even cause a shift in the cellular response pattern to TNF. Tumor cells that are fully resistant to sTNF-TNF-R1-mediated cytotoxicity become highly vulnerable and are killed through TNF-R2-dependent activation upon presentation of memTNF (9). However, this superior capacity of full TNF-R2-activation to initiate cellular responses is not restricted to direct cytotoxicity against tumor cells. TNF-R2 also confers typical TNF responses in local inflammatory processes (6). TNF-R2 binding leads to significantly higher expression levels of T lymphocyte HLA-DR proteins or endothelial tissue factor (11), stimulates macrophages more efficiently to defend invading microorganisms (12), and optimizes activation of the respiratory burst of polymorphonuclear leukocytes (PMN) (13).

Considering the broad range of the multiple memTNF-dependent effector mechanisms, the use of its bioactivity as an anticancer agent is a promising therapeutic approach. However, minimizing TNF toxicity to normal tissue would require both the prevention of systemic soluble TNF-like action and the locally restricted enrichment of memTNF activity to the tumor compartment. Concerning epithelial cancers, the tumor compartment consists of two discrete, but interdependent, components, the malignant cells and the tumor stroma. The predominant cells in the tumor stroma are nontransformed fibroblasts, expressing the genetically stable fibroblast-activating protein (FAP) in >90% of all cases (14). The FAP-positive stromal cells commonly contribute 50–90% of the tumor mass and are located in close vicinity to the endothelial cells of the tumor capillaries and surround the tumor nodules. Focusing the bioactivity of memTNF to the FAP-positive tumor stroma should therefore promote the antitumor efficacy of the cytokine at several

*Medical Department I, Universität des Saarlandes, Homburg/Saar, Germany; †Ludwig Institute for Cancer Research, Memorial Sloan Kettering Cancer Center, New York, NY 10158; and ‡Ludwig Institute for Cancer Research Austin and Repatriation Medical Center, Heidelberg, Victoria, Australia

Received for publication July 25, 2003. Accepted for publication January 20, 3004.

The costs of publication of this article were defrayed in part by the payment of page charges. This article must therefore be hereby marked *advertisement* in accordance with 18 U.S.C. Section 1734 solely to indicate this fact.

[1] This work was supported in part by Grant 10-1812-ReI from the Deutsche Krebshilfe.

[2] Address correspondence and reprint requests to: Dr. Christoph Renner, Medical Department I, Saarland University Medical School, Kirrberger Strasse, D-66421 Homburg/Saar, Germany. E-mail address: incren@uniklinik-saarland.de

[3] Abbreviations used in this paper: memTNF, transmembrane TNF; FAP, fibroblast-activating protein; HC, H chain; KRPG, Krebs-Ringer phosphate with glucose; LC, L chain; PECAM-1, platelet endothelial cell adhesion molecule-1; PMN, polymorphonuclear leukocyte; rh, recombinant human; sTNF, soluble TNF; TF, tissue factor.

0022-1767/04/$02.00

levels. 1) Reflecting the fact that endothelial cells are the major target for TNF-mediated hemorrhagic tumor necrosis, the FAP-dependent enrichment of TNF in a memTNF-like manner should initiate enhancement of endothelial tissue factor production by cooperative TNF-R signaling. 2) The TNF-initiated induction of adhesion molecules on the luminal surface of the tumor vessels should favor Ag-neighbored adherence of PMNs and trigger the release of reactive oxygen species, causing stromal tissue damage. 3) Furthermore, not only FAP-positive cells, but also the 4) malignant cells in their proximity, could activate autoproteolytic programs, even under conditions where a phenotypic switch of the cellular response pattern should have to be induced to become susceptible.

To direct these memTNF-induced cellular response programs to the FAP-positive tumor stroma, we established an Ab fusion protein that consists of the humanized anti-FAP Ab (15) and human TNF. The TNF sequence started at aa 79 of the precursor protein and was blocked through direct linkage to the IgG1 hinge region. The CH2/CH3 region of the human IgG1 Fc portion was replaced by the human TNF sequence to prevent nonspecific binding to FcRs. This type of linkage should provide a certain rigidity of the fusion protein, thus mimicking the membrane-anchored presentation of TNF via Ab-mediated specific binding to FAP. Furthermore, the design of the TNF compound as a dimer should minimize any FAP-independent systemic activity of sTNF, which physiologically signals as a compact trimer.

Our in vitro and in vivo data demonstrate that the fusion protein exhibits an effector profile identical with that of memTNF associated with up to 10-fold reduced toxicity compared with sTNF, proving that the Ab-linked TNF dimer is an optimal transmitter of memTNF bioactivity.

Materials and Methods

Cell lines and reagents

RPMI 1640 medium (supplemented with 10% (v/v) heat-inactivated FCS, penicillin (100 U/ml), streptomycin (0.1 mg/ml), and glutamine (0.3 mg/ml); all from Life Technologies, Karlsruhe, Germany) was used as standard medium. HT1080 FAP-transfected (HT1080 FAP) and mock-transfected (HT1080 par) cells were supplied by Boehringer Ingelheim (Biberach, Germany). WEHI-164 S (TNF-sensitive) and WEHI-164 R (TNF-resistant) cells were cultured in standard medium as previously described (16). Colo205 was obtained from American Type Culture Collection (Manassas, VA). HUVEC-c endothelial cell-supplemented growth medium was obtained from PromoCell (Heidelberg, Germany). Human recombinant TNF and soluble TNF-R1 were purchased from Genzyme (Neu-Isenburg, Germany). Rat anti-mouse CD11b (clone M1/70) and rat anti-mouse platelet endothelial cell adhesion molecule-1 (PECAM-1; clone MEC13.3) were purchased from BD PharMingen (San Diego, CA). Biotinylated goat anti-human IgG was a component of the Vectastain ABC kit (Vector Laboratories, Burlingame, CA), biotinylated rabbit anti-mouse $F(ab)_2$ and goat anti-rat IgG $F(ab)_2$ were obtained from Dianova (Hamburg, Germany). Infliximab was purchased from Centocor (Leiden, Netherlands), Etanercept from Whyeth Pharma (Munster, Germany), and murine anti-idiotypic anti-FAP from Boehringer Ingelheim. The anti-G250 mAb was provided by Prof. S. Warnaar (Pathology Department, University of Leiden, Leiden, The Netherlands).

RT-PCR

RT-PCR of mRNA isolated from PBMC was performed as previously described (7). Amplification of the mature human TNF cDNA sequence was performed using the following primer pairs: 5′-ATCACCATGGTCT CATCTTCTCGAACCCCGAGTG-3′ and 5′-AGTTTCTAGATCACAGG GCAATGATCCCAAAGTAG-3′.

Amplification of variable Ab sequences

The cDNA sequence coding for the variable H (HC) and L (LC) chain sequences of the humanized anti-FAP Ab was amplified as previously described (7). The respective cDNA template of the humanized anti-FAP Ab was provided by Boehringer Ingelheim, and the following primer pairs were used: HC reverse, 5′-CAGGTTTAAACGCCGCCACCATGGACT GGACCTGGCGCGTGTTTTGC-3′; HC forward, 5′-CAGGGATCCAC TCACCTGAGGAGACGGTGAC-3′; LC reverse, 5′-CAGGAAATTTC GCCGCCACCATGGAGACAGACACACTCCTGCTATGG-3′; and LC forward, 5′-CAGGGATCCACTCACGTTTTATTTCCACCTTGGTCCC CTG-3′.

Generation of eukaryotic expression vectors

A eukaryotic expression vector system (pREN) with either human constant IgG1 HC or κ LC sequences under the control of the elongation factor α promoter was used for recombinant protein expression. Variable HC and LC sequences were inserted by restriction digest (*Pme*/*Bam*HI) into the corresponding pREN vector. The pREN HC vector was modified by inserting an *Nco*I site in-frame after the hinge region to insert the TNF cDNA fragment (anti-FAP-TNF HC). Methotrexate resistance was incorporated into the HC vector, and neomycin resistance was incorporated into the LC vector.

Generation of stable transfected cell lines and Ab production

Stable transfected CHO cell lines were established by electroporation using a GenPulser (Bio-Rad, Munich, Germany). In brief, 400 μl of cells (1×10^7/ml) were mixed with 10 μg of circular DNA, electroporated (270 V, 975 μF), and plated out in a volume of 150 ml of medium. G418 selection (0.5 mg/ml; Life Technologies, Karlsruhe, Germany) commenced after 2 days, methotrexate (5 nM; Wyeth, Münster, Germany) was added on day 7 and increased to 100 nM over 2 wk. Stable cell lines producing high levels of Abs were expanded, weaned off FCS, and transferred into a Technomouse system (Integra Biosciences/Technomara, Fernwald, Germany) for large scale production.

Purification and biochemical characterization of recombinant Abs

Technomouse-derived Ab supernatant was dialyzed against PBS (pH 7.2) overnight (4°C) and passed over a protein L-Sepharose column (fast protein liquid chromatography system; Amersham Pharmacia Biotech, Freiburg, Germany). Binding Abs were eluted stepwise by adding 0.1 M glycine/HCl (pH 3.5), and samples were neutralized rapidly by the addition of 1 M Tris buffer (pH 8.0). Molecular mass determination of native immunocytokine was performed with a Superdex 200 prep grade HiLoad 16/60 using low and high gel filtration chromatography calibration kits (ferritin, 460 kDa; catalase, 206 kDa; aldolase, 107 kDa; albumin, 67 kDa; OVA, 43 kDa; chymotrypsinogen A, 25 kDa; Amersham Pharmacia Biotech). The elution volumes were determined from the chromatogram, and the calibration curve of calculated K_{av} values vs the log m.w. was generated. The m.w. of anti-FAP-IgG1 TNF dimer was obtained from analysis of the calibration curve. SDS-PAGE analysis was performed as described previously (17), and protein bands were visualized by staining with Coomassie Brilliant Blue (Sigma-Aldrich, Munich, Germany). Proteins were transferred to a polyvinylidene difluoride membrane (Millipore, Bedford, MA) for Western blotting analysis, and membranes were blocked with 10% nonfat dry milk before incubating with rabbit anti-human TNF (1/1000), followed by goat anti-rabbit IgG conjugated to HRP (1/3000; Bio-Rad, Munich, Germany), and were developed by chemiluminescence (ECL kit; Amersham Pharmacia Biotech).

Binding analysis

Flow cytometry was performed as described previously (17). In brief, 1×10^6 tumor cells were incubated with purified Abs with the indicated specificity and concentration (30 min, 4°C). Cells were washed twice with PBS and incubated with rabbit anti-TNF (1/1000 dilution, 30 min, 4°C; DAKO, Hamburg, Germany), and finally, the complex was visualized by adding PE-conjugated goat anti-rabbit serum (1/100 dilution; DAKO). Ten thousand cells of each sample were counted and analyzed.

Binding of anti-FAP-IgG1-TNF was also assessed by ELISA. Ninety-six-well, flat-bottom microtiter plates (MaxiSorp Immuno microwell plates; Nunc, Roskilde, Denmark) were coated (overnight, 4°C) with Infliximab (1 μg/ml), Etanercept (1 μg/ml), or recombinant human TNF-R1 (rhTNF-R1; 1 μg/ml) in 50 μl of coating buffer/well. Plates were blocked with 1.5% gelatin in PBS, and then the indicated reagents resolved in PBS were added in serial dilutions (1 h, room temperature). After incubation with murine anti-idiotypic anti-FAP Ab (1 μg/ml, 1 h, room temperature), biotinylated rabbit anti-mouse serum (1/2000, 1 h, room temperature) and HRP (1/50,000, 15 min, room temperature; Roche, Mannheim, Germany) were added. Plates were developed by the addition of *o*-phenylenediamine substrate (Sigma-Aldrich, Deisenhofen, Germany). The reaction was

stopped with 3 M HCl, and plates were read on a Fluorometer (model 1420, Victor 2; Wallac, Turku, Finland) at 490 nm.

Preparation of human PMN and measurement of H_2O_2 release

PMN were purified from venous blood of healthy donors as previously described (18). All H_2O_2 measurements were performed in flat-bottom microtiter plates (MaxiSorp Immuno microwell plates; Nunc) using the plate-reading fluorometer (18). Plates were precoated with 1 μg/ml human plasma fibronectin (Harbor Bio-Products, Norwood, MA) in 50 μl of Krebs-Ringer phosphate with glucose (KRPG)/well (37°C, 2 h) in a humidified incubator (5% CO_2). Before use, plates were washed three times with PBS and prewarmed to 37°C, and then 100 μl of KRPG containing 50 μM A6550 (Molecular Probes, Eugene, OR) and 1 U/ml HRP (Sigma-Aldrich; reaction mixture) were added. Triggering agents and Abs were added thereafter in 10 μl of KRPG/well. Plates were incubated (37°C, 10 min), and the reaction was started by the addition of 3×10^4 PMN in 20 μl of KRPG to each well. Measurements were made at selected time points (37°C over 120 min in air). H_2O_2 standard curves with A6550 were generated in parallel, and fluorescence changes from the activated PMN were converted to nanomolar concentrations of H_2O_2 using these standard curves.

Cytotoxicity and proliferation assays

Different methods were used for the detection of cell death. One way of assessing dead cells was the annexin V-biotin method according to the manufacturer's recommendation (Roche). In brief, tumor cells (5×10^5) were cultured in 24-well plates overnight in the presence of the indicated amount of Abs or human TNF, washed in PBS, and then incubated with annexin V-biotin (10 μl) in reaction buffer (10 mM HEPES/NaOH (pH 7.4), 140 mM NaCl, and 5 mM $CaCl_2$). After 15 min, cells were washed, and the percentage of annexin V-FITC-positive cells was determined by flow cytometry as described above. Assays were repeated at least three times. For analysis of memTNF-mediated cytotoxicity, Colo205 target cells were cocultured with FAP-transfected or mock-transfected FAP-negative HT1080 cells (2×10^4/well). Experiments with the Colo205 clone were performed as previously described (9). In brief, the HT1080 clones were seeded in microtiter plates overnight and incubated with the indicated amounts of Abs (30 min, 4°C). After washing with PBS, cells were fixed with 2% formaldehyde (10 min, 37°C) and washed three times with PBS before the Colo205 cells were added (2×10^4/well). The viability of the target cells was measured after 48 h using the EZ4U assay (Biomedica, Wien, Austria) according to the manufacturer's instructions at 492 nm. Absorbance of untreated cells defined 100% viability.

Tissue factor activity of HUVECs

The HUVEC endothelial cells were prepared as previously described (19) and cultured in supplemented growth medium. Cells were detached from the culture dish by EDTA treatment (0.5 mM) and scraping. The assay was conducted with whole cells in suspension at second or third passage. Tissue factor (TF) activity was assessed by monitoring the hydrolysis of chromogenic substrate S-2222 (Chromogenix, Milan, Italy) as previously described (9, 20). In brief, 1×10^5 endothelial cells were seeded in triplicate with 2×10^5 FAP-positive or -negative HT1080 cells and preincubated (30 min, 4°C) with the indicated amounts of reagents. After coincubation (4 h, 37°C), HUVECs were washed, and reaction buffer (50 mM HEPES, 100 mM NaCl, 5 mM $CaCl_2$, 0.5% BSA, 10 mM FVIIa (American Diagnostica, Greenwich, CT), and 100 mM FX (American Diagnostica), pH 7.4) was added. FXa formation was assessed using 400 μM S-2222. Hydrolysis was monitored at 37°C by measuring the change in absorbance at 405 nm. A standard curve with upper and lower detection limits of 25 and 0.395 ng/ml was generated using lipidated human recombinant TF.

Immunohistochemistry

Mice were sacrificed, and xenotransplanted solid tumors together with a margin of surrounding tissue were harvested. Excised samples were snap-frozen in liquid nitrogen and stored at −80°C. Sections were cut and placed on SuperFrost Plus microscope slides (Menzel-Glaser, Braunschweig, Germany). For staining, slides were fixed in cold acetone, air-dried, rehydrated in PBS, and then blocked using a Biotin Blocking System (DAKO, Carpinteria, CA). Before adding the primary Ab (anti-mouse CD11b or anti-mouse PECAM-1, 1/100), slides were blocked with healthy human donor serum (Vectastain ABC Kit; Vector Laboratories, Burlingame, CA). For staining with humanized/chimeric Abs (anti-human FAP, anti-human G250, or irrelevant isotype-matched human IgG; 1/5000), slides were blocked with FCS (1/100). The biotinylated secondary Ab (goat anti-human IgG (1/200) or goat anti-rat IgG (1:1000)) and the preformed avidin-biotinylated HRP complex (ABC reagent) were used according to the manufacturer's instructions. The Ab-ABC complex was visualized with a 3-amino-9 ethylcarbazole (Sigma-Aldrich, St. Louis, MO)-based chromagen, resulting in a pink-brown coloration of Ag-positive cells. All slides were counterstained with Meyer's hematoxylin.

Tumor model and treatment protocols

Adult male and female BALB/c *nu/nu* mice (6–8 wk old; Charles River Laboratories, Wilmington, MA) were used for toxicity and efficacy assessment. Tumor engraftment to analyze FAP expression on tumor cells in vivo was achieved by s.c. injection of 2×10^6 FAP-transfected HT1080 cells in the right flank. This cell number was known to achieve a 100% take rate (data not shown). FAP Ag expression on xenografts was confirmed every 8 days over 4 wk (two mice per time point). In the first experimental setting, 15 animals were divided randomly into three experimental groups (five mice per group), and treatment was initiated when solid tumors had reached ~5 mm^3. Two treatment groups received equal doses (100 μg suspended in 150 μl of PBS) of anti-FAP-IgG1-TNF dimer or of the parental anti-FAP Ab administered i.v. by tail vein injection every 3 days for five consecutive injections. Control mice received the same volume of PBS alone. Health and body weight were monitored daily, whereas tumor size measurements were assessed on treatment days. Animals were sacrificed when tumor volume reached >1 cm^3. The second model relied on the simultaneous establishment of HT1080-FAP-positive and parental, mock-transfected Ag-negative (HT1080 par) xenografts on opposing flanks in the same mice. Cells of each cell line (2×10^6; suspended in 150 μl of PBS) were injected s.c. into the right or left flank, respectively. Fifteen simultaneous FAP-positive and -negative tumor-bearing animals were then divided into five groups of three and treated in the same manner. Tumor growth and body weight were again monitored closely. The final in vivo experiment was performed with an identical protocol design compared with the second model. Treatment, however, was extended by the application of rhTNF and anti-G250-TNF dimer (our unpublished observations) to characterize the specificity of effector recruitment and to define maximum tolerated doses. All studies were performed under an existing animal ethics approval as required by federal law.

Results

Generation of the CH2/CH3-truncated dimerized anti-FAP-IgG1-TNF fusion protein

In the present immunocytokine, the CH2/CH3 of the human Fc region has been replaced by the mature human TNF molecule, resulting in the formation of a TNF dimer stabilized by the natural disulfide bond IgG1 hinge region. The variable domains of the humanized anti-FAP Ab were inserted through specific restriction sites, and the final fully human vector construct was confirmed by DNA sequencing. High level expression of the recombinant immunocytokine in CHO cells was achieved with a final yield of 15 mg/liter of culture. The immunocytokine was purified in the current study using a one-step procedure on protein L columns. Analysis of purified anti-FAP-IgG1-TNF dimer by size exclusion fast protein liquid chromatography showed that the immunocytokine migrated at ~150 kDa (Fig. 1*A*). Furthermore, the purity and integrity of the eluted material were analyzed by gel electrophoresis under reducing and nonreducing conditions and Western blotting (Fig. 1*B*). The recombinant H chain product (anti-FAP-HC) is slightly smaller than a natural IgG1 H chain and runs at 47 kDa. The human L chain is not altered and has a size of 28 kDa.

Binding assays

Target Ag binding of the immunocytokine was assessed by flow cytometry and compared with its parental anti-FAP Ab counterpart. At all Ab concentrations ranging from 10 μg/ml to 10 ng/ml, comparable binding properties regarding affinity and specificity were observed without any significant difference (Fig. 2*A*). Binding of the anti-FAP-TNF construct was demonstrated on HT1080-FAP^+ cells using an anti-human TNF-α Ab. Furthermore, correct biochemical assembly of the TNF moiety was analyzed by ELISA, demonstrating proper binding to Infliximab (chimeric anti-human

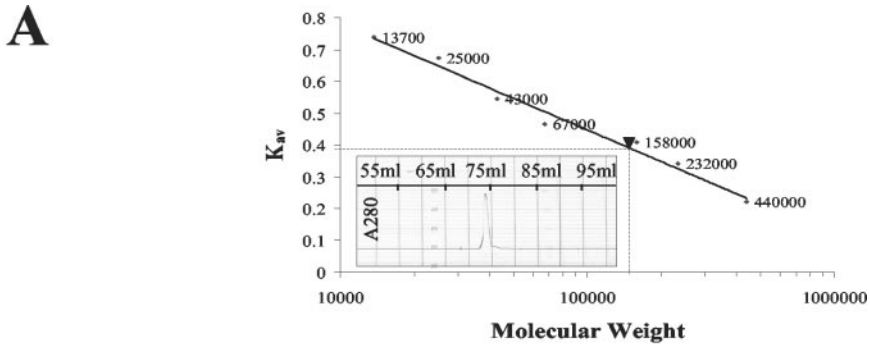

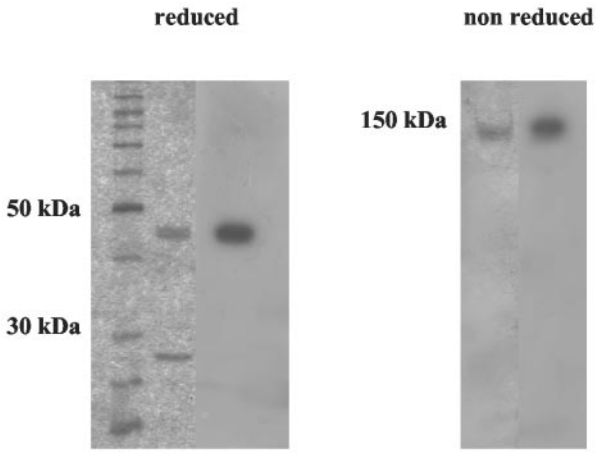

FIGURE 1. Biochemical characterization of the anti-FAP-IgG1-TNF dimer. *A*, Fast protein liquid chromatographic molecular mass determination of native immunocytokine (▼). The molecular mass of anti-FAP-IgG1 TNF dimer was 150 kDa on elution compared with those of the indicated standards. The gel filtration profile included in the figure demonstrates the corresponding peak, consistent with the dimeric format of the Ab construct. *B*, SDS-PAGE analysis (reducing and nonreducing conditions) with Coomassie staining (*left*) and Western blot (*right*) detection via rhTNF-specific serum of the purified fusion protein.

TNF mAb), rhTNF-R1, or Etanercept (rhTNF-R2-Fc fusion protein), respectively. Binding of the anti-FAP-TNF dimer was visualized using a murine anti-idiotypic anti-FAP Ab (Fig. 2, *B–D*) to prove the integrity of the entire construct.

Reduced soluble TNF-like cytotoxic activity of the anti-FAP-TNF dimer

In the first instance, WEHI-164 cells were used to investigate the sTNF-like activity of the anti-FAP-TNF dimer in comparison with that of the parental FAP Ab and trimerized rhTNF. Using annexin V as a very sensitive indicator of cell death, a strong correlation between the concentration of the anti-FAP-TNF construct and the level of cell killing was observed. Specific cell lysis was detected down to concentrations of 1 pg/ml for the anti-FAP-TNF dimer. However, a significantly stronger cell lysis was seen for commercially available recombinant rhTNF (~10-fold). Neither medium alone nor the parental anti-FAP Ab at the highest concentration (10 μg/ml) induced a significant level of cell death. A WEHI-164 variant cloned under the exposure to TNF was partially resistant to both rhTNF and the anti-FAP-TNF construct (Fig. 3*A*). Coincubation with Etanercept inhibited the anti-FAP-TNF-mediated lysis of TNF-sensitive WEHI-164 cells, whereas an irrelevant IgG control Ab failed to block TNF-activity (Fig. 3*B*).

H_2O_2 release in response to anti-FAP-TNF dimer

It has been widely demonstrated that human PMN release large quantities of reactive oxygen species in response to TNF when the cells are adherent to surfaces coated with extracellular matrix proteins. Fig. 4 shows the respiratory burst of human PMN adherent on fibronectin-coated plates measured as H_2O_2 production. Addition of the anti-FAP-TNF construct resulted in high superoxide production, whereas the parental anti-FAP Ab induced an effect comparable to that of KRPG buffer. Responses induced by anti-FAP-TNF dimer were similar to those to rhTNF.

Membrane-anchored TNF-like cytotoxic activity mediated by anti-FAP-TNF dimer

The assays described above proved the potency of the dimerized cytokine to act like sTNF. However, the anti-FAP-TNF dimer was designed to achieve targeted bioactivity of memTNF via both TNF-R types after binding to the FAP Ag. For that purpose the anti-FAP-TNF construct was absorbed to FAP-positive or -negative cells, and the unbound Ab was washed off and then added to WEHI-164 cells. As expected, only the immunocytokine attached to FAP-positive HT1080 cells was able to mediate a strong and concentration-dependent lysis of WEHI target cells (Fig. 5*A*). No

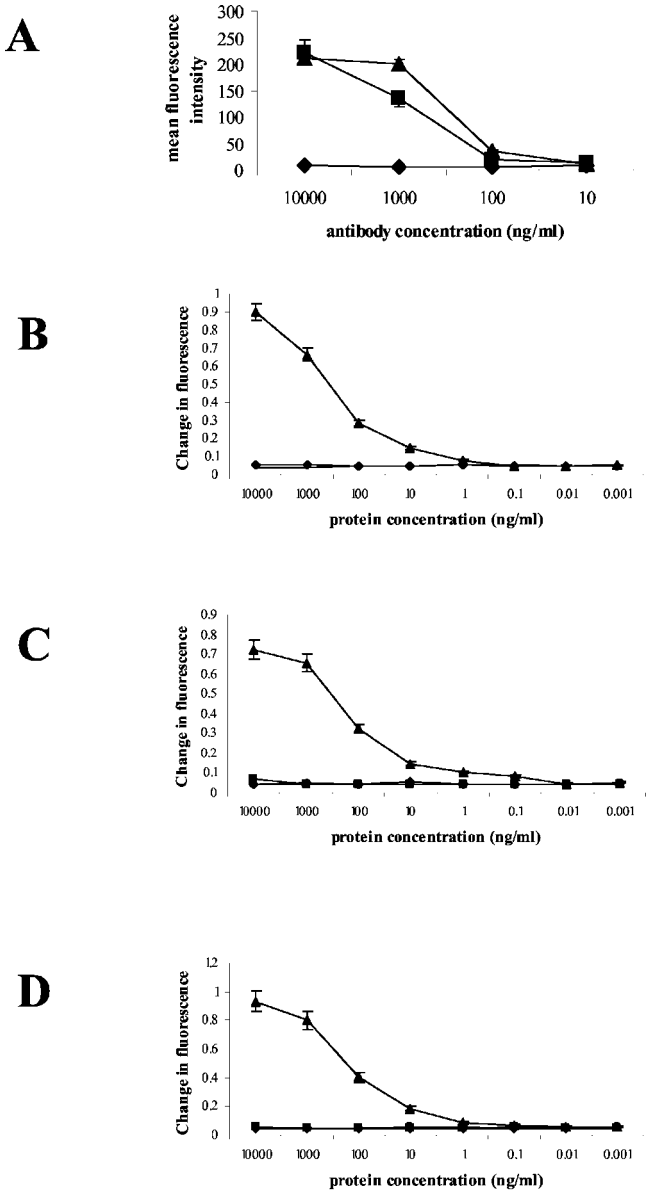

FIGURE 2. Binding properties of the anti-FAP-TNF dimer and parental anti-FAP Ab. *A*, Cell surface binding was determined by FACScan analysis using the FAP-transfected HT1080 cell line as the target. The mean fluorescence intensity of binding of the indicated amounts of Ab (anti-FAP-TNF (▲), parental anti-FAP (■), and chimeric anti-CD30 (♦)) were analyzed. Assays were performed in triplicate. No specific binding could be detected on FAP Ag-negative tumor cells or the parental HT1080 cell line, respectively (data not shown). *B–D*, Binding of the anti-FAP-TNF dimer to coated TNF-R1 (*B*), Etanercept (*C*), or Infliximab (*D*) was detected by ELISA. The anti-TNF/immunocytokine complexes were visualized by a murine anti-idiotypic anti-FAP mAb. The anti-FAP TNF dimer (▲) built stable complexes with both immobilized anti-TNF agents. Parental anti-FAP (■), anti-G250 TNF dimer (♦), and rhTNF (●) served as controls.

such activity was detected when the parental HT1080 cell line (mock-transfected, FAP Ag-negative) or parental anti-FAP Ab were used. To investigate the ability of the immunocytokine to induce additive cytotoxicity via TNF-R2-dependent signaling by mimicking the memTNF message, a second experiment was performed. In contrast to the WEHI-164 S clone, Colo205 cells are completely resistant to the cytotoxic activity of sTNF, even at high concentrations. Only by memTNF-like signaling did Colo205 cells become highly susceptible to TNF-mediated autoproteolysis (9).

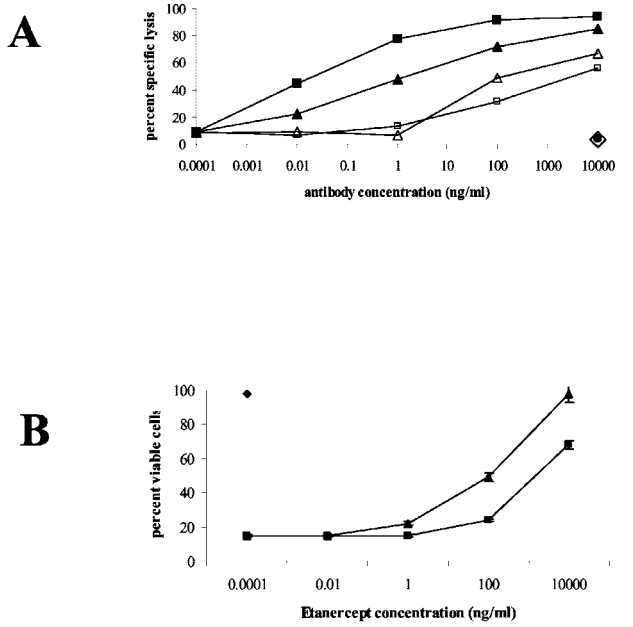

FIGURE 3. Cytotoxic activity of the anti-FAP-TNF construct on WEHI-164 cells. *A*, TNF-sensitive (WEHI-164-S; ■ and ▲) or TNF-resistant (WEHI-164-R; □ and △) cells were incubated with the indicated reagents (anti-FAP-TNF dimer (▲ and △) and parental anti-FAP Ab (◇)) or rhTNF (■ and □) for 12–18 h. Medium alone (♦) served as the negative control, and the number of dead cells was analyzed by annexin V binding. *B*, WEHI-164-S cells were incubated for 12–18 h with 100 ng/ml of the effector proteins (anti-FAP-TNF dimer (▲), parental anti-FAP Ab (♦), or rhTNF (■)) in the presence of the indicated amounts of Etanercept. Coincubation with Etanercept inhibited the lysis of TNF-sensitive target cells.

The anti-FAP-TNF dimer exhibited memTNF-like activity via presentation by FAP-expressing HT1080 cells to the Colo205 line, resulting in a dose-dependent measurable death of the target cells. The control samples including coincubation of FAP-negative HT1080 cells with the fusion protein, the unbound anti-FAP-TNF dimer alone, or the FAP-bound parental Ab failed to induce lysis of the Colo205 cells, respectively (Fig. 5*B*).

Membrane-anchored TNF-like induction of endothelial tissue factor expression by anti-FAP-TNF dimer

One of the main tumoricidal mechanisms of TNF represents the alteration of tumor vasculature leading to subsequent tumor necrosis. The central step to initiate this thrombotic process involves enhanced synthesis and surface expression of endothelial TF. Stimulation of HUVEC with memTNF leads to a significantly higher TF expression compared with sTNF (9, 11). We determined the induction of TF expression on HUVECs by the anti-FAP-TNF dimer acting either in solution or presented in cell-bound status via FAP Ag by a two-step chromogenic assay. The saturated concentration of sTNF leading to highest TF expression was 35 ng/ml, in accordance with previously reported data (9). Under these conditions, coincubation of HUVECs with FAP-expressing HT1080 cells alone or with FAP-negative HT1080 cells in the presence or the absence of anti-FAP-TNF dimer failed to induce increased TF synthesis. However, increasing amounts of TF activity, despite saturated sTNF concentration, were detectable after coincubation of HUVECs with FAP-expressing HT1080 cells preincubated with anti-FAP-TNF dimer (Fig. 6).

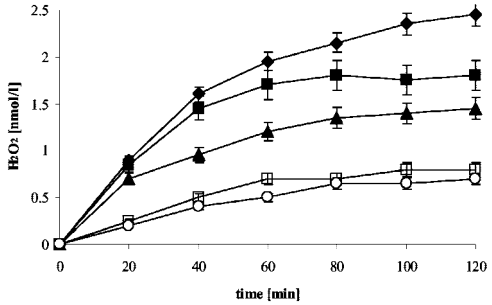

FIGURE 4. Granulocyte activation induced by anti-FAP Ab constructs in solution. Granulocyte activity was determined using an H_2O_2 release assay with adherent human granulocytes (PMN). Stimulation was performed with 1 μg/ml anti-FAP-TNF dimer (■) or parental anti-FAP-mAb (□), 1 μg/ml rhTNF (▲), or no stimulus (○). PMA (♦; 15 ng/ml) served as a positive control. A representative experiment of three similar ones, each conducted in triplicate, is reported.

In vivo toxicity of anti-FAP-TNF dimer

BALB/c *nu/nu* mice bearing FAP^+ solid human fibrosarcoma xenografts (~5 mm^3) were treated with a total of five consecutive injections, each 3 days apart, to analyze the in vivo toxicity and activity of the anti-FAP-TNF fusion protein. To compare equimolar concentrations, 30 μg of human TNF was compared with 100 μg of anti-FAP-TNF. The group of tumor-bearing mice treated with 30 μg of rhTNF all died within 24 h and could not be challenged with a second injection. Mice treated with the immunocytokine, however, showed some signs of stress, but all completed treatment without any lethal side effects. The anti-FAP-TNF immunocytokine administered five times at 100 μg/injection did not cause significant weight loss when only one solid tumor had been established per mouse (Fig. 7). When animals were challenged simultaneously with the FAP Ag-positive and -negative cell lines, however, all animals lost weight over time regardless of their treatment. The effect on weight loss was most pronounced in the group of mice treated with repetitive doses of the anti-FAP-TNF immunocytokine, but was still minor (Fig. 7).

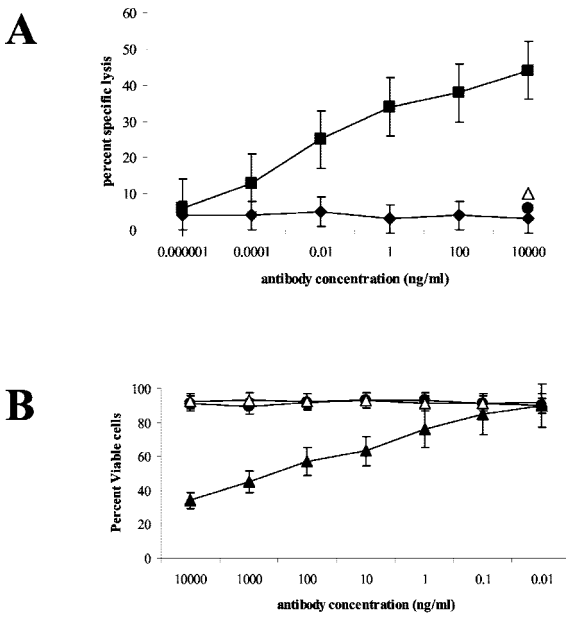

FIGURE 5. Activity of anti-FAP-TNF dimer loaded onto tumor cells. FAP-transfected (■) and mock-transfected (♦) HT1080 cells were incubated with the indicated amount of anti-FAP-TNF Ab. Cells were then washed in medium (*A*) and mixed with fluorescence dye-labeled WEHI-164-S cells. The percentage of annexin V-positive WEHI-164-S cells was determined by flow cytometry. Parental anti-FAP Ab (◇) and culture medium (●) served as controls. Ten thousand cells were analyzed per sample, and the mean fluorescence intensity was determined. *B*, Coculture of FAP-transfected (▲ and ●) or FAP-negative HT1080 cells (△) with Colo205 in the presence of parental anti-FAP Ab (●) or anti-FAP-IgG1-TNF dimer (▲ and △).

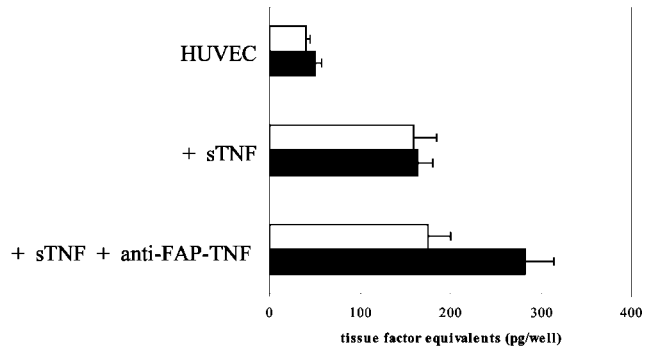

FIGURE 6. Anti-FAP-TNF dimer-mediated induction of endothelial tissue factor. HUVECs were cocultured with FAP-transfected (■) or FAP-negative (□) HT1080 cells (4 h) in the absence or the presence of saturated concentrations of sTNF before surface expression of TF was measured as described in *Materials and Methods*. Anti-FAP-TNF dimer was added at a concentration of 1 μg/ml; an irrelevant immunocytokine (G250-TNF) had no effect (data not shown). Values represent the means of triplicate determinations.

In vivo activity of the anti-FAP-TNF dimer

Previous experiments had shown that the HT1080-FAP^+ cell line is, per se, not TNF sensitive and can only be lysed in vitro by our construct or human TNF, respectively, in the presence of cycloheximide (data not shown). In addition, established FAP^+ fibrosarcomas were only poorly vascularized (Fig. 9*B*), thus limiting both the intratumoral uptake of the fusion protein and the antitumor effects mediated through TNF activity on endothelial cells. Therefore, the major focus of this animal model was on toxicity

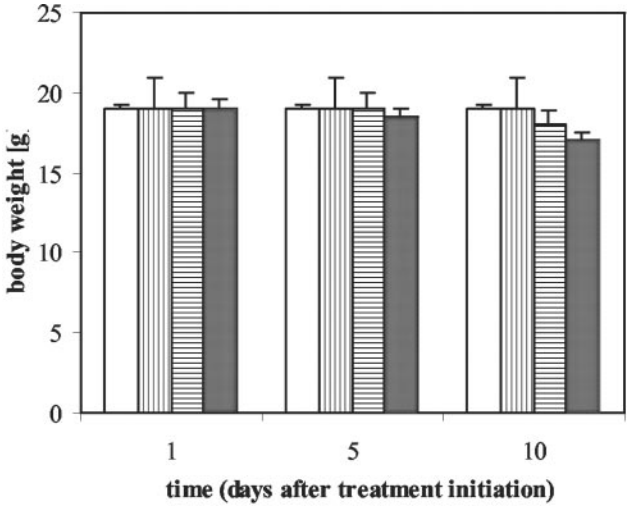

FIGURE 7. Effect of treatment on body weight of BALB/c *nu/nu* mice. Mice bearing single FAP-positive (□ and ▥) or simultaneously positive and negative xenografts (▤ and ▩) were treated with either buffer (□ and ▤) or the anti-FAP TNF dimer (100 μg/injection; ▥ and ▩), and body weight was measured at the indicated time points.

induced by our construct in comparison with equimolar concentrations of rhTNF. Nevertheless, the repeated i.v. injection of 100 μg of anti-FAP-TNF dimer caused a significant delay of tumor growth (Fig. 8*A*). Control animals treated with the parental anti-FAP Ab, a control immunocytokine with no FAP specificity, or PBS alone, respectively, showed no growth inhibition. To demonstrate that the antitumor effect of the anti-FAP-TNF dimer is Ag dependent, we established simultaneously HT1080-FAP$^+$ (FAP-positive) and HT1080 par (FAP-negative) tumor xenografts on opposite flanks of the same mice (Fig. 8*B*). Tumor-bearing animals underwent the same regimen as in the first experiment. Application of the anti-FAP-TNF dimer again caused regression of the FAP-positive fibrosarcomas in the same manner, whereas mock-transfected tumor cells lacking FAP expression were not affected in their growth pattern. Immunohistological analysis of anti-FAP-TNF-treated tumors demonstrated a strong accumulation of murine PMNs in FAP-expressing tumors (Fig. 9*A*). Staining of tumor sections showed a solid mass of tumor cells without significant vessel structures assessed by immunohistochemistry using the endothelial cell marker PECAM-1. Vessel structures that stained positively for PECAM-1 were restricted to the outer connective tissue capsule surrounding the tumor (Fig. 9*B*). To clarify that the induction and extent of PMN enrichment were triggered by targeted delivery of the TNF fusion protein, we performed an additional xenograft study. Animals bearing FAP-positive and -negative tumors were challenged with an increasing dose regimen. In an analogy to former treatment, equal doses (100 μg), but increasing numbers of injections, were administered every 3 days. Tumors were harvested 24 h after the last injection for immunohistochemical analysis. The enrichment of anti-CD11b-stained murine leukocytes in the targeted tissue corresponded to the injected cumulative dose of the anti-FAP TNF dimer (Fig. 9, *C* and *E*). Again, fusion protein-mediated PMN recruitment was strictly Ag dependent (Fig. 9, *D* and *F*), as detection of leukocytes surrounding FAP-negative tissue failed (Fig. 9*G*), and treatment of animals with the parental anti-FAP Ab did not result in leukocyte homing (Fig. 9*H*). Furthermore, effector cell recruitment to FAP$^+$ tissue could not be achieved by application of dimerized TNF coupled to an Ab with irrelevant Ag-specificity (anti-G250-TNF dimer; Fig. 9*I*).

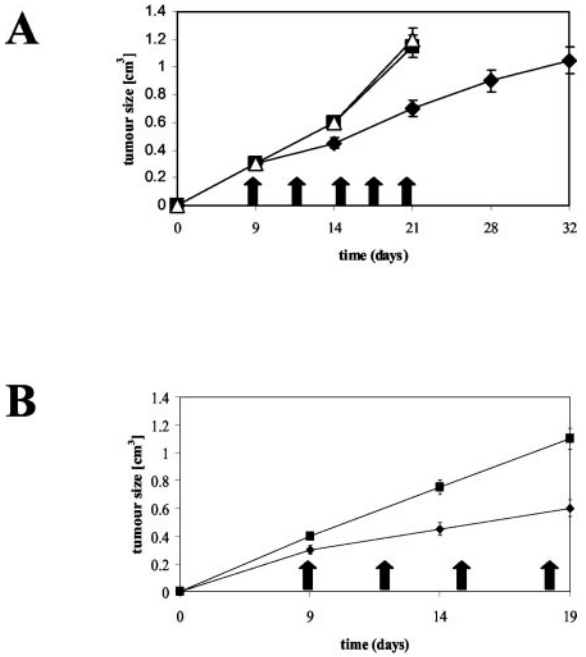

FIGURE 8. Effects of TNF immunocytokine on the growth pattern of tumor xenografts. *A*, FAP-positive tumors were established in BALB/c *nu/nu* mice as described, and mice were randomly assigned to different treatment groups on day 9. One hundred micrograms of the Abs (anti-FAP-TNF (♦) and parental anti-FAP (■)) or of buffer alone (△) were injected i.v. every 3 days as indicated (↑). The growth delay on day 21 reached significance ($p < 0.005$) for the immunocytokine group. Animals were removed from the study when tumor volume exceeded 1 cm^3. *B*, Delay of tumor growth as a consequence of Ag expression. Simultaneous growth of two phenotypically different xenografts (FAP-positive (♦) and FAP-negative (■)) in nude mice was achieved as described, and animals were assigned to their respective treatment groups when tumor diameter reached 5 mm. Again, animals were treated with repetitive i.v. applications of the immunocytokine (100 μg/injection) as indicated (↑). Animals had to be removed from the study on day 19 because the volume of the FAP-negative xenograft exceeded 1 cm^3. At this time point the difference in tumor size between FAP-positive and -negative xenografts was significant ($p < 0.01$).

Discussion

In the present study we describe a new human immunocytokine targeting tumor stroma by binding to the FAP Ag and delivering membrane-anchored TNF-α bioactivity. We have deliberately chosen the IgG1-hinge-TNF Ab format because a CH2/CH3-deleted fusion protein has some advantages compared with similar approaches where the cytokine moiety is attached behind the CH3 domain (21). The latter construct resembles an intact IgG1 Ab with the cytokine at the C-terminal end. The resulting tetravalent Ab constructs maintain most of their Fc region-associated effector functions, such as long half-life and FcR binding (22). Accordingly, one would expect that a TNF fusion protein derived from an intact IgG1 Ab would bind to unprimed macrophages and induce the typical signal pattern of sTNF (23). As a consequence, systemic side effects and unfavorable tumor-targeting properties should limit the clinical use of such a compound. The CH2/CH3-deleted fusion protein described by us has no known FcR-binding properties (data not shown). The truncation left the hinge region unaffected to ensure the stability of the fusion protein. Blocking the N-terminal TNF domain through direct linkage to the hinge region even increases rigidity and reinforces the final fusion protein to retain the character of a dimeric protein, because mature TNF monomers associate intimately to form a solid state. However, this raises the question of the general activity of the TNF portion of the immunocytokine. Data from the literature dealing with deletion of the first amino acid residues of native TNF either reported no influence on the activity or even a 4-fold increase (24). Another important question concerns the dimeric structure of the TNF component, because a 3-fold symmetry of TNF and TNF-R superfamilies physiologically defines the essential signaling stoichiometry and structure (25).

In addition to recent data demonstrating the superior capacity of memTNF when acting in a positive cooperative manner through both TNF-R forms, a TNF-R2-specific mAb was developed that was able to mimic the activity of memTNF in the presence of sTNF (9). Adjacent kinetic studies revealed that this Ab stabilized the receptor/ligand binding, leading to a prolonged half-life of the complex. The authors raised the hypothesis that the intracellular signaling strength could depend on the kinetics of receptor-ligand complex formation, because the rapid dissociation of sTNF from TNF-R2 failed to induce intracellular signals (9). Subsequent studies showed that the agonistic activity of this Ab was dependent on its dimeric IgG1 structure, as Fab were inactive (26). The fact that dimerization of TNF-R2 is an obligatory step for the initiation of the signal cascades (27) also suggests that the secondary clustering of the TNF-TNF-R2 complexes by this Ab could reflect the responsible mechanism for enhanced memTNF-TNF-R2 signaling

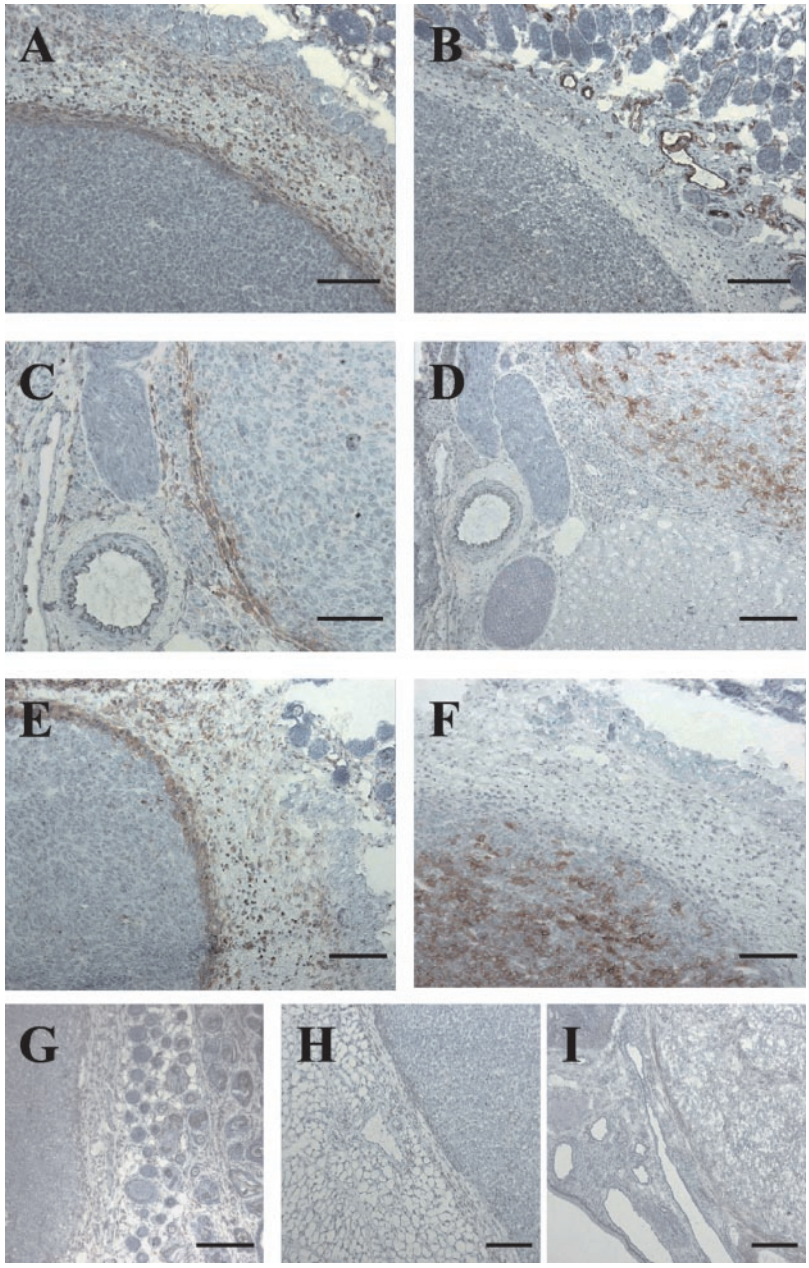

FIGURE 9. Specific effector cell recruitment to FAP-positive tumors by treatment with anti-FAP-TNF dimer. Tumors were immunohistochemically stained for $CD11b^+$ effector cells (PMN; *A*) and $PECAM\text{-}1^+$ vessels (*B*) in anti-FAP-TNF-treated mice. To demonstrate dose-dependency of PMN accumulation, mice were treated with a dose-increasing regimen as described, and tumor tissue was harvested 24 h after i.v. application of one dose of 100 μg (*C* and *D*) or three doses of 100 μg (*E* and *F*) of anti-FAP-TNF dimer. PMN accumulation was visualized again by anti-CD11b staining (*C* and *E*) adjacent to FAP-positive tumors (*D* and *F*). PMN recruitment could not be demonstrated for the parental anti-FAP Ab (*G*) or simultaneously established FAP-negative tumors when treated with the anti-FAP-TNF Ab (*H*). In addition, an unrelated anti-G250-TNF dimer failed to induce any antitumor response (*I*). For all slides, 100-fold optical magnification was used. Final slide adjustment was performed using Adobe Photoshop Elements (Adobe Systems, Unterschleissheim, Germany). Bars indicate 1 mm.

capacity. Consequently, the extent of TNF-R2 signaling is not solely determined by the affinity of the receptor-ligand interaction (28). This is in accordance with our finding that the anti-FAP-TNF dimer binds to Etanercept (Fig. 2*B*), a fusion protein made up of the extracellular domain of TNF-R2 and the hinge and Fc domain of human IgG1 (29). Complexes of an anti-FAP-TNF dimer and Etanercept were more stable over time compared with an anti-FAP single-chain Ab genetically fused to rhTNF monomer (data not shown). Together this might explain why the anti-FAP-IgG1-TNF dimer in the current study exerts the bioactivity of memTNF, although the dimerized structure causes a reduced affinity for TNF-R1 (30) compared with recombinant soluble TNF (Fig. 3). Furthermore, the induction of intracellular death domain signaling pathways via TNF-R1, including those leading to apoptosis, is based on internalization of the ligated receptor complex (31). The 150-kDa size of our fusion protein could sterically hamper this endocytosis. In contrast to TNF-R1-induced apoptotic pathways, the responses of PMNs to TNF-triggered respiratory burst are probably not dependent upon receptor complex internalization, because the proline-rich tyrosine kinase (pyk2) that plays a critical role in this activation process is not linked to the death domains of TNF-R1. Therefore, known inhibitors of TNF-R1 endocytosis could not block the kinase activity (31, 32). The enzyme acts by integrating the TNF and β_2 integrin signals, whereas the cooperation of TNF-R2 in the respiratory burst-inducing process is more important at low TNF concentrations, suggesting a modulatory role at physiologically relevant concentrations of the cytokine (6). This is in accordance with our data and explains the equal extent of H_2O_2 release after stimulation with rhTNF or in response to our fusion protein, as all reagents acted in solution on adherent human PMNs (Fig. 4). Again, this argues for the importance of the CH2/CH3 deletion in our IgG1 fusion protein to prevent TNF-induced triggering of peripheral blood macrophages subsequent to FAP-independent FcR binding.

To date, our results confirmed the expected behavior of the IgG1 fusion protein when acting in solution. The challenged activity

profile, however, included induction of the memTNF-TNF-R2-mediated signal capacity. In several coculture assays, the FAP Ag-bound fusion protein showed the juxtatropic cytotoxicity of cell surface TNF that signals by cell-to-cell contact (Figs. 5 and 6). We chose the Colo205 assay to demonstrate that our construct could be responsible for a strong signal enhancement by inducing stabilization of TNF-TNF-R2 complexes. The induction of cell death by TNF-R2 signaling in Colo205 cells reflected the memTNF-like activity of the anti-FAP-IgG1-TNF dimer, resulting in IgG1-dependent receptor clustering (Fig. 5*B*). Further evidence for the potency of the construct to initiate TNF-R2-dependent pathways was shown by TF induction on HUVEC. Both TNF-Rs are involved in TNF responses resulting in the expression of this endothelial prothrombotic factor (11). However, under conditions of saturated concentrations of sTNF acting through TNF-R1, only additional signaling through TNF-R2 yields superior rates of TF expression (9). Again, presentation of the anti-FAP-TNF construct in its Ag-bound status to the human endothelial cells resulted in memTNF bioactivity leading to enhanced cell surface expression of TF (Fig. 6). This is the key event for the activation of the extrinsic coagulation cascade resulting in thrombotic infarction of tumors. Destruction of tumor vessels is the major effect of TNF when used in isolated limb perfusion as the only clinically accepted use for rhTNF (33). To overcome this restriction of TNF application for tumor immunotherapy, the advantage of our construct with regard to reduced toxicity in vivo had to be demonstrated, because after i.v. application the TNF-portion of the fusion protein could potentially interact with the type I TNF-R of nontargeted cells, above all endothelial cells, despite Ab linkage. This stimulation could increase vascular permeability and finally lead to capillary leak syndrome (34, 35). As FAP expression of transfectants was detectable over 4 wk of solid growth in BALB/c *nu/nu* mice (data not shown), in vivo targeting of FAP-transfected HT1080 cells provided an appropriate test system to examine the toxicity profile of the fusion protein. Human TNF in its trimeric structure is ~30-fold less active in BALB/c *nu/nu* mice than its murine homologue (36) with a calculated 50% lethal dose of 1.2 μg for recombinant mouse TNF and 20–30 μg for rhTNF, respectively (37). Therefore, we decided to use single injections of 30 μg of human TNF to achieve proposed 50% lethal dose level. As expected, all animals treated died within 24 h. However, mice treated with 100 μg of anti-FAP-TNF dimer/injection did not die and could be treated repetitively. Only mice bearing xenografts of the FAP Ag-negative and -positive HT1080 cell line simultaneously experienced significant weight loss and cachexia. Nevertheless, it is well known from the literature that tumor-bearing animals are more susceptible to TNF-mediated kachexia (38).

The animal model was not designed primarily to demonstrate antitumor efficacy, because rhTNF fails to induce murine TNF-R2 signaling (39), but the cooperative signaling through both TNF-Rs represents the therapeutic principle of the anti-FAP-TNF dimer, exerting its antitumor activity in a membrane TNF-like manner. Therefore, drug-related therapeutic events should be expected via TNF-R1 (35). As stated above, the HT1080 FAP^+ cell line is not TNF sensitive, and we could not expect to induce tumor cell apoptotis by our construct. Furthermore, the growth pattern of xenotransplanted fibrosarcoma was characterized by poor vascularization, thus excluding fusion protein-mediated TNF signaling leading to endothelial TF up-regulation causing hemorrhagic tumor necrosis. Finally, the respiratory burst of mouse neutrophils in response to soluble TNF is 10-fold lower than that for their human counterparts (40, 41). However, when established xenografts were treated from day 9 after tumor inoculation, a significant delay in tumor growth was observed. Immunohistochemical analysis revealed FAP Ag-dependent recruitment of murine leukocytes as the main effector mechanism, exclusively induced by anti-FAP-TNF dimer. This was a reliable and dose-dependent inducible effect. In addition, we confirmed the fusion protein-mediated growth delay in a second experiment in which mice had mock-transfected FAP Ag-negative and -positive tumor xenografts established simultaneously. Again, the FAP-positive tumors revealed delayed growth after anti-FAP-TNF treatment, with no change in the growth pattern for the FAP-negative tumors established on the opposite flank of the mouse.

In conclusion, we present data on a TNF-based immunocytokine that exerts its Ag-restricted therapeutic activity after i.v. injection with tolerable systemic toxicity. The anti-FAP-TNF dimer gains the potent bioactivity of memTNF exclusively after binding to the target Ag and initiates various cellular response programs. Focusing the described synergistic antitumor activities to the FAP-positive tumors minimized in vivo side effects. Two previous studies have described the concept of CH2/CH3 truncation to design Ab hybrid molecules similar to ours, but never achieved production levels that allowed them to perform relevant assays (42, 43). Our genetically engineered construct reached production yields of 15 mg/liter. A transition into good manufacturing practice-conforming desired production processes should be feasible and guarantee the initiation of clinical trials (44).

Acknowledgments

We thank Anja Reich and Nicole Jordan for excellent technical assistance. We thank the Department of Clinical and Experimental Surgery for housing and handling of animals.

References

1. Old, L. J. 1987. Tumor necrosis factor: polypeptide mediator network. *Nature 326:330*.
2. Kriegler, M., C. Perez, K. De Fay, I. Albert, and S. D. Lu. 1988. A novel form of TNF/cachectin is a cell surface cytotoxic transmembrane protein: ramifications for the complex physiology of TNF. *Cell 53:45*.
3. Wajant, H., and P. Scheurich. 2001. Tumor necrosis factor receptor-associated factor (TRAF) 2 and its role in TNF signaling. *Int. J. Biochem. Cell. Biol. 33:19*.
4. Grell, M., G. Zimmermann, E. Gottfried, C.-M. Chen, U. Grünwald, D. C. S. Huang, Y.-H. W. Lee, H. Dürkop, H. Engelmann, P. Scheurich, et al. 1999. Induction of cell death by tumor necrosis factor (TNF) receptor 2, CD40 and CD30: a role for TNF-R1 activation by endogenous membrane-anchored TNF. *EMBO J. 18:3034*.
5. Beutler, B., and F. Bazzoni. 1998. TNF, apoptosis and autoimmunity: a common thread? *Blood Cells Mol. Dis. 24:216*.
6. Perez, C., I. Albert, K. DeFay, N. Zachariades, L. Gooding, and M. Kriegler. 1990. A nonsecretable cell surface mutant of tumor necrosis factor (TNF) kills by cell-to-cell contact. *Cell 63:251*.
7. Bauer, S., C. Renner, J.-P. Juwana, G. Held, S. Ohnesorge, K. Gerlach, and M. Pfreundschuh. 1999. Immunotherapy of human tumors with T-cell-activating bispecific antibodies: stimulation of cytotoxic pathways in vivo. *Cancer Res. 59:1961*.
8. Ratner, A., and W. R. Clark. 1993. Role of TNF-α in $CD8^+$ cytotoxic T lymphocyte-mediated lysis. *J. Immunol. 150:4303*.
9. Grell, M., E. Duoni, H. Wajant, M. Löhden, M. Clauss, B. Maxeiner, S. Georgopoulos, W. Lesslauer, G. Kollias, K. Pfizenmaier, et al. 1995. The transmembrane form of tumor necrosis factor is the prime activating ligand of the 80kDa tumor necrosis factor receptor. *Cell 83:793*.
10. Weingärtner, M., D. Siegmund, U. Schlecht, M. Fotin-Mleczek, P. Scheurich, and H. Wajant. 2002. Endogenous membrane tumor necrosis factor (TNF) is a potent amplifier of TNF receptor 1-mediated apoptosis. *J. Biol. Chem. 38:34853*.
11. Schmidt, E. F., K. Binder, M. Grell, P. Scheurich, and K. Pfizenmaier. 1995. Both tumor necrosis factor receptors, $TNFR_{60}$ and $TNFR_{80}$, are involved in signaling endothelial tissue factor expression by juxtacrine tumor necrosis factor α. *Blood 86:123*.
12. Birkland, T. P., J. P. Sypek, and D. J. Wyler. 1992. Soluble TNF and membrane TNF expressed on $CD4^+$ T-lymphocytes differ in their ability to activate macrophage antileishmania defense. *J. Leukocyte Biol. 51:296*.
13. Dri, P., E. Haas, R. Cramer, R. Menegazzi, C. Gasparini, R. Martinelli, P. Scheurich, and P. Patriarca. 1999. Role of the 75-kDa TNF receptor in TNF-induced activation of neutrophil respiratory burst. *J. Immunol. 162:460*.
14. Garin-Chesa, P., L. J. Old, and W. J. Rettig. 1990. Cell surface glycoprotein of reactive stromal fibroblasts as a potential antibody target in human epithelial cancers. *Proc. Natl. Acad. Sci. USA 87:7235*.
15. Scott, A. M., G. Wiseman, S. Welt, F. T. Lee, W. Hopkins, P. Mitchell, A. Adjei, C. Divgi, S. Larson, E. Hoffman, et al. 2001. A phase I dose-escalation study of

BIBH1 in patients with advanced or metastatic fibroblast activation protein positive cancer. *Proc. Am. Soc. Clin. Oncol. 20: 258a.*
16. Espevik, T., and J. Nissen-Meyer. 1986. A highly sensitive cell line, WEHI 164 clone 13, for measuring cytotoxic factor / tumor necrosis factor from human monocytes. *J. Immunol. Methods 95:99.*
17. Renner, C., W. Jung, U. Sahin, R. van Lier, and M. Pfreundschuh. 1995. The role of lymphocyte subsets and adhesion molecules in T cell-dependent cytotoxicity mediated by CD3 and CD28 bispecific monoclonal antibodies. *Eur. J. Immunol. 25:2027.*
18. Mohanty, J. G., J. S. Jaffe, E. S. Schulman, and D. G. Raible. 1997. A highly sensitive fluorescent micro-assay of H_2O_2 release from activated human leukocytes using a dihydroxyphenoxazine derivative. *J. Immunol. Methods 202:133.*
19. Jaffe, E. A., R. L. Nachman, C. G. Becker, and C. R. Minick. 1973. Culture of human endothelial cells derived from umbilical veins. *J. Clin. Invest. 52:2745.*
20. Carson, S. D. 1987. Continuous chrommogenic tissue factor assay: comparison to clot-based assays and sensitivity established using pure tissue factor. *Thromb. Res. 47:379.*
21. Christ, O., S. Seiter, S. Matzku, C. Burger, and M. Zoller. 2001. Efficacy of local versus systemic application of antibody-cytokine fusion proteins in tumor therapy. *Clin. Cancer Res. 7:985.*
22. Coloma, M. J., and S. L. Morrison. 1997. Design and production of novel tetravalent bispecific antibodies. *Nat. Biotechnol. 15:159.*
23. Watson, F., L. Gasmi, and S. W. Edwards. 1997. Stimulation of intracellular $Ca2^+$ levels in human neutrophils by soluble immune complexes: functional activation of FcγRIIIb during priming. *J. Biol. Chem. 272:17944.*
24. Guo, D., B. Shen, X. Dong, Q. Qiu, and X. Xu. 1995. Creation of a high cytotoxic active human tumor necrosis factor having the truncated and more basic amino terminus. *Biochem. Biophys. Res. Commun. 207:927.*
25. Locksley, R. M., N. Killeen, and M. J. Lenardo. 2001. The TNF and TNF receptor superfamilies: integrating mammalian biology. *Cell 104:487.*
26. Krippner-Heidenreich, A., F. Tübing, S. Bryde, S. Willi, G. Zimmermann, and P. Scheurich. 2002. Control of receptor-induced signaling complex formation by the kinetics of ligand/receptor interaction. *J. Biol. Chem. 277:44155.*
27. Grell, M., P. Scheurich, A. Meager, and K. Pfizenmaier. 1993. TR60 and TR80 Tumor necrosis factor (TNF)-receptors can independently mediate cytolysis. *Lymphokine Cytokine Res. 12:143.*
28. Grell, M., H. Wajant, G. Zimmermann, and P. Scheurich. 1998. The type I receptor (CD120a) is the high affinity receptor for soluble tumor necrosis factor. *Proc. Natl. Acad. Sci. USA 95:570.*
29. Scallon, B., A. Cai, N. Solowski, A. Rosenberg, X.-Y. Song, D. Shealy, and C. Wagner. 2002. Binding and functional comparisons of two types of tumor necrosis factor antagonists. *J. Pharmacol. Exp. Ther. 301:418.*
30. Petersen, C. M., A. Nykjaer, B. S. Christiansen, L. Heickendorff, S. C. Mogensen, and B. Moller. 1989. Bioactive human recombinant tumor necrosis factor-α: an unstable dimer? *Eur. J. Immunol. 19:1887.*
31. Schütze, S., T. Machleidt, D. Adam, R. Schwandner, K. Wiegmann, M.-L. Kruse, M. Heinrich, M. Wickel, and M. Krönke. 1999. Inhibition of receptor internalization by monodansylcadaverine selectively blocks p55 tumor necrosis factor receptor death domain signaling. *J. Biol. Chem. 274:10203.*
32. Han, H., M. Fuortes, and C. Nathan. 2003. Critical role of the carboxyl terminus of proline-rich tyrosine kinase (Pyk2) in the activation of human neutrophils by tumor necrosis factor: separation of signals for the respiratory burst and degranulation. *J. Exp. Med. 197:63.*
33. Ruegg, C., A. Yilmaz, G. Bieler, J. Bamat, P. Chaubert, and F. J. Lejeune. 1998. Evidence for the involvement of endothelial cell integrin $\alpha_V\beta a_3$ in the disruption of the tumor vasculature induced by TNF and IFN-γ. *Nat. Med. 4:408.*
34. Curnis, F., A. Sacchi, L. Borgna, F. Magni, A. Gasparri, and A. Corti. 2000. Enhancement of tumor necrosis factor α antitumor immunotherapeutic properties by targeted delivery to aminopeptidase (CD13) *Nat. Biotechnol. 18:1185.*
35. Ferrero, E., M. R. Zocchi, E. Magni, M. C. Panzeri, F. Curnis, C. Rugarli, M. E. Ferrero, and A. Corti. 2001. Roles of tumor necrosis factor p55 and p75 receptors in TNF-α-induced vascular permeability. *Am. J. Physiol. 281:C1173.*
36. Smith, R. A., M. Kirsteiun, W. Fierst, and C. Baglioni. 1986. Species specificity of human and murine tumor necrosis factor. *J. Biol. Chem. 261:14871.*
37. Kramer, S. M., B. B. Aggarwal, T. E. Eessalu, S. M. McCabe, B. L. Ferraiolo, I. S. Figari, and M. A. Palladino, Jr. 1988. Characterization of the in vitro and in vivo species preference of human and murine tumor necrosis factor α. *Cancer Res. 48:920*
38. Krosnick, J. A., J. K. McIntosh, J. J. Mule, and S. A. Rosenberg. 1989. Studies of the mechanisms of toxicity of the administration of recombinant tumor necrosis factor α in normal and tumor-bearing mice. *Cancer Immunol. Immunother. 30:133.*
39. Ameloot, P., W. Fiers, P. De Bleser, C. F. Ware, P. Vandenabeele, and P. Brouckaert. 2001. Identification of tumor necrosis factor (TNF) amino acids cruical for binding to the murine p75 TNF receptor and construction of receptor-selective mutants. *J. Biol. Chem. 40:37426.*
40. Lowell, C. A., L. Fumagalli, and G. Berton. 1996. Deficiency of Src family kinases $p59/61^{hck}$ and $p58^{c\text{-}fgr}$ results in defective adhesion-dependent neutrophil functions. *J. Cell Biol. 133:895.*
41. Yaffe, M. B., J. Xu, P. A. Burke, R. A. Forse, and G. E. Brown. 1999. Priming of the neutrophil respiratory burst is species dependent and involves MAP kinase activation. *Surgery 126:248.*
42. Hoogenboom, H. R., J. C. Raus, and G. Volckaert. 1991. Targeting of tumor necrosis factor to tumor cells: secretion by myeloma cells of a genetically engineered antibody-tumor necrosis factor hybrid molecule. *Biochim. Biophys. Acta 1096:345.*
43. Xiang, J., T. Moyana, and Y. Qi. 1997. Genetic engineering of a recombinant fusion possessing anti-tumor $F(ab')_2$ and tumor necrosis factor. *J. Biotechnol. 53:3.*
44. Scott, A. M., D. Geleick, M. Rubira, K. Clarke, E. C. Nice, F. E. Smyth, E. Stockert, E. C. Richards, F. J. Carr, W. J. Harris, et al. 2000. Construction, production, and characterization of humanized anti-Lewis Y monoclonal antibody 3S193 for targeted immunotherapy of solid tumors. *Cancer Res. 60:3254.*